Progressive Macula Vessel Density Loss in Primary Open Angle Glaucoma: A Longitudinal Study

Takuhei Shoji[1,2], **Linda M. Zangwill**[1], **Tadamichi Akagi**[1,3], **Luke J. Saunders**[1], **Adeleh Yarmohammadi**[1], **Patricia Isabel C. Manalastas**[1], **Rafaella C. Penteado**[1], and **Robert N. Weinreb**[1]

[1]Hamilton Glaucoma Center, Shiley Eye Institute, and Department of Ophthalmology, University of California San Diego, La Jolla, California

[2]Department of Ophthalmology, Saitama Medical University, Iruma, Saitama, Japan

[3]Department of Ophthalmology and Visual Sciences, Kyoto University Graduate School of Medicine, Kyoto, Japan

Abstract

Purpose—To characterize the rate of macula vessel density loss in primary open angle glaucoma (POAG), glaucoma suspect, and healthy eyes.

Design—Longitudinal, observational cohort from the Diagnostic Innovations in Glaucoma Study.

Methods—One hundred eyes (32 POAG, 30 glaucoma suspect and 38 healthy) followed for at least one year with optical coherence tomography angiography (OCT-A) imaging on at least two visits were included. Vessel density was calculated in the macula superficial layer. The rate of change was compared across diagnostic groups using multivariate linear mixed-effects model.

Results—Baseline macula vessel density was highest in healthy eyes, followed by glaucoma-suspect and POAG eyes (P < 0.01). The rate of vessel density loss was significantly different from zero in the POAG, but not in the glaucoma suspect or healthy eyes. The mean rate of change in macula whole en-face vessel density was significantly faster in glaucoma eyes (−2.23 %/yr) than in glaucoma suspect (0.87%/yr, P = 0.001) or healthy eyes (0.29 %/yr, P = 0.004). Conversely, the rate of change in ganglion cell complex (GCC) thickness was not significantly different from zero in any diagnostic group, and no significant differences in the rate of GCC change among diagnostic groups were found.

Conclusions—With a mean follow-up of less than 14 months, eyes with POAG had significantly faster loss of macula vessel density than either glaucoma suspect or healthy eyes. Serial OCT-A measurements also detected glaucomatous change in macula vessel density in eyes without evidence of change in GCC thickness.

Introduction

Primary open angle glaucoma (POAG) is a progressive optic neuropathy and a leading cause of worldwide blindness. The role, if any, of impairment in ocular blood flow and alterations of the retinal microvasculature continues to be debated. [1–6]

Numerous technologies have been used to study the relationship between the retinal microvasculature and glaucoma progression including fluorescein angiography (FA), [7] indocyanine green angiography,[8] scanning laser ophthalmoscopy angiography,[9] laser Doppler flowmetry [10–12] and laser speckle flowgraphy.[13] However, the study of ocular microcirculation in glaucoma has been problematic due to the inability to directly observe clearly the microvasculature within discrete layers of the retina and optic nerve head.[3] Moreover, it has not been possible to obtain their accurate, reproducible and quantitative measurement.[3] The recent introduction of optical coherence tomography angiography (OCT-A) addresses these limitations and offers the potential for enhancing our understanding of the role in glaucoma of ocular blood flow and the retinal microvasculature.

OCT-A enables study of the superficial and the deep retinal vessels, including those in the macula region.[14–16] Moreover, specialized software (split-spectrum amplitude-decorrelation angiography - SSADA) quantitatively and reproducibly assesses the retinal microvasculature.[17–19] In a previous study, OCT-A measurement of peripapillary vessel density within the RNFL distinguished glaucoma eyes from healthy and suspect ones [20, 21]. Moreover, a significant relationship between vessel density and the severity of visual field damage was observed.[22] Investigations of OCT-A vessel density to date have largely evaluated in cross-sectional studies the peripapillary region, and there only is sparse information about macula vessel density.

The macula is among the most metabolically active of all human tissues and derives its oxygen supply from multiple retinal capillary plexuses.[23, 24] About one half of the retinal ganglion cell soma are concentrated in the macula.[25, 26] They depend on regional capillary networks to meet their high metabolic requirements. Rao et al. reported that parafoveal vessel density was significantly lower in glaucoma than in healthy eyes.[27] In their study, the diagnostic accuracy of parafoveal vessel density was only moderate, and lower than the diagnostic accuracy of peripapillary vessel density in differentiating glaucoma from healthy eyes. [27] It is not known, however, whether changes in macula vessel density are detectable over time.

The purpose of the current study was to compare the longitudinal changes of the vessel density measurements within the superficial macula of glaucoma, glaucoma-suspect and healthy eyes using OCT-A. We also compared the rates of macula vessel density changes to the rates of ganglion cell complex thinning measured with spectral domain OCT (SD-OCT).

Methods

This was a prospective, longitudinal observational study. Participants were recruited from the Diagnostic Innovations in Glaucoma Study (DIGS) (ClinicalTrials.gov identifier, NCT00221897). [28] This study was approved by the Institutional Review Board of the University of California, San Diego (UCSD), and conformed to the tenets of the Declaration of Helsinki and the Health Insurance Portability and Accountability Act. Written informed consent was obtained from all participants.

Participants

Healthy subjects, glaucoma suspects, and primary open angle glaucoma (POAG) patients enrolled in DIGS with longitudinal OCT-A imaging (Angiovue; Optovue Inc., Fremont, CA)[15, 17, 20, 22, 29–31] and SD OCT imaging (Avanti; Optovue Inc., Fremont, CA). Details of the DIGS protocol and patient eligibility have been described previously.[28] In brief, all participants completed a comprehensive ophthalmological examination, including best-corrected visual acuity, slit-lamp biomicroscopy, intraocular pressure (IOP) measurement by Goldmann applanation tonometry, gonioscopy, dilated fundus examination, stereoscopic optic disc photography, ultrasound pachymetry, and standard automated perimetry (SAP) in both eyes. Only participants with open angles on gonioscopy, and spherical refraction within ± 10 diopters were included. Subjects aged 45 years who had at least 2 visits with good quality OCT-A imaging examinations and with at least 12 months of follow-up were eligible for inclusion in this report.

Healthy subjects were required to have an IOP of 21 mmHg or less, with no history of elevated IOP, normal-appearing optic discs, intact neuroretinal rims and retinal nerve fiber layer (RNFL), and a normal visual field test results within 6 months of OCT-A imaging. A normal visual field was defined as a pattern standard deviation (PSD) within the 95% confidence limits, and a Glaucoma Hemifield Test within normal limits.

Glaucoma-suspects had an IOP 22 mmHg or suspicious-appearing optic discs without evidence of repeatable glaucomatous visual field damage. Glaucomatous visual field damage was defined by the presence of repeatable abnormal visual field results with glaucoma hemifield test results outside normal limits or PSD outside the 95% normal limits.

Eyes were classified as glaucomatous if they had repeatable glaucomatous visual field damage defined as a GHT outside normal limits and PSD outside 95% normal limits. Glaucoma suspects were defined as having glaucomatous optic neuropathy or suspicious appearing optic discs based on stereo photograph reviewed by two experienced graders and/or ocular hypertension (IOP > 21 mm Hg) without evidence of repeatable glaucomatous visual field damage.

Participants with a history of intraocular surgery (except for uncomplicated cataract surgery or glaucoma surgery), coexisting retinal pathologies, non-glaucomatous optic neuropathy, uveitis, or ocular trauma were excluded from the study. Participants were also excluded if there was a diagnosis of Parkinson's disease, Alzheimer's disease, dementia, or a history of stroke. Participants with systemic hypertension and diabetes mellitus were included, unless

they were diagnosed with diabetic or hypertensive retinopathy. Participants with an unreliable visual field, or poor quality OCT-A images or SD-OCT scans, were also excluded from this report.

Systemic blood pressure (BP) was measured twice on the day of the baseline visit using the Omron Automatic (Model BP791IT; Omron Healthcare, Inc., Lake Forest, IL, USA) blood pressure instrument. Mean arterial pressure was calculated as one-third systolic BP + two-thirds diastolic BP. Mean ocular perfusion pressure (MOPP) was defined as the difference between two-thirds of mean arterial pressure and the IOP.

Standard Automated Perimetry

All participants underwent visual field testing using the 24-2 pattern Swedish interactive threshold algorithm on the Humphrey Field Analyzer (Carl Zeiss Meditec, Dublin, CA, USA) within 6 months of OCT-A imaging. Only reliable tests (33% fixation losses and false negatives, and 15% false-positives) were included. The quality of visual field tests was also reviewed by the Visual Field Assessment Center[32] staff to identify and exclude visual fields with evidence of inattention or inappropriate fixation, artifacts, such as eyelid and lens rim artifacts, fatigue effects, and abnormal results caused by diseases other than glaucoma.

Optical Coherence Tomography Angiography

The AngioVue is an angiographic platform implemented on an existing commercially available SD-OCT platform. The OCT-A AngioVue imaging system provides both structural and vascular measurements. The image acquisition technique was optimized for the Split-Spectrum Amplitude-Decorrelation Angiography algorithm, which has been described in detail.[17] The SSADA method captures the dynamic motion of moving particles, such as red blood cells flowing in a blood vessel, and allows high-resolution 3-dimensional visualization of perfused vasculature. OCT-A characterizes vascular information at each retinal layer as an en-face angiogram, a vessel density map, and quantitatively, as vessel density, calculated as the percentage area occupied by flowing blood vessels in the selected region.

Binary images of vascular networks were created using an automated thresholding algorithm. Vessel density was summarized for the whole, superior, and inferior en-face image regions of the superficial retinal capillary plexuses (SCP) of the macula. More specifically, we used vessel density measurements within the macula, in scans with a $3.0 \times 3.0\text{-mm}^2$ field of view centered on the fovea. En-face OCT angiograms with 304×304-pixel dimensions were produced by maximum decorrelation (i.e., flow) projection between the segmentation lines. Each scan was automatically segmented by the AngioVue software (version 2015.1.0.90) in order to visualize the superficial retinal capillary plexuses (SCP) and deep retinal capillary plexuses (DCP) of the retina. Based on these default settings, the SCP en-face OCT-A image was segmented with an inner boundary set at 3 μm below the internal limiting membrane, and an outer boundary set at 15 μm below the inner plexiform layer. Vessel density was calculated as the whole en-face image, which was divided by a horizontal line into 2 sectors, i.e., the superior and inferior en-face regions and over the foveal and parafoveal regions. The sectors were defined based on the Early Treatment

Diabetic Retinopathy Study (ETDRS) sectors, where the fovea center was automatically determined from the relevant OCT data. Parafoveal vessel density was measured in an annular region with an inner diameter of 1.0 mm and outer diameter of 2.5 mm centered on the fovea. The foveal region was defined as a central circle and the parafoveal region was defined as circular annulus centered on the macula. The parafoveal region was also divided into 4 sectors of 90° each (nasal, inferior, superior, and temporal sectors) (Figure 1). We analyzed SCP, as it corresponds to the ganglion cell complex (GCC), an established measure for assessing glaucoma detection. [33] Trained graders reviewed the quality of all OCT-A scans using a standard protocol established by the Imaging Data Evaluation and Analysis (IDEA) reading center at UCSD. Poor-quality scans were excluded from the analysis if 1 of the following criteria were met: (1) signal strength index (SSI) of <45 (1 = minimum, 100 = maximum); (2) poor-clarity images; (3) local weak signal caused by artifacts such as floaters; (4) residual motion artifacts visible as irregular vessel patterns or disc boundary on the enface angiogram; and (5) images with off-center fovea. During the follow-up period, scans with best and worst SSI values differing by more than 15 were also excluded.

Spectral-Domain OCT Imaging

All subjects completed macula cube imaging with a commercially available spectral-domain (SD-) OCT system (Avanti) which consisted of a70-kHz axial line rate, 840-nm central wavelength, and an axial resolution of 5-μm in tissue. The macula scanning protocol was utilized to measure the GCC (i.e. the combined thickness of the RNFL, ganglion cell layer (GCL), and inner plexiform layer (IPL)) thickness. The center of the GCC scan is shifted 0.75 mm temporally to improve sampling of the temporal periphery. Only good quality images, as defined by scans with a signal strength index   40, and without segmentation failure and artifacts were included. The overall average GCC thickness, global loss volume (GLV) and focal loss volume (FLV) were used in this analysis.

OCT-A and SD-OCT images were obtained by the same operator and at the same visit using the AngioVue, which is a dual modality OCT system.

Statistical Analysis

The data are expressed as the mean ± standard deviation (SD) for continuous variables and frequencies (percentages) for categorical variables. Categorical variables were compared using the chi-square test. Analysis of variance (ANOVA) and post-hoc Tukey honest significant differences were calculated to compare mean measurements between healthy, glaucoma suspect, and glaucoma eyes. The number of visits, MD, PSD and rate of vessel density change (%/year) were not normally distributed using the Shapiro–Wilk W test. So these parameters were expressed as the median (25,75 percentile) and compared using the nonparametric Kruskal–Wallis test with post hoc Dunnet multiple comparisons. We used mixed effects modeling to estimate the rates of vessel density and GCC loss/change in each group (healthy vs glaucoma suspect vs glaucoma). Models were fit with macula vessel density measurements as response variable with time, diagnostic group and a time diagnostic group interaction as fixed effects. The glaucoma diagnostic group x time interaction term indicates the difference between eyes in each diagnostic group in estimated rate of change of vessel density over time, and the P value shows the significance of the difference. We used

random intercepts and random slopes to account for repeated measurements over time with eyes nested within subject to account for the fact that eyes from the same individual are more likely to have similar measurements. [34, 35] The models were refitted with other possible predictors that were borderline significant predictors (p < 0.1) of measurement magnitude in univariate models to adjust the analysis for these variables. Age, central corneal thickness, axial length, SSI, blood pressure (systolic, diastolic and mean), calculated mean ocular perfusion pressure, and IOP were among the covariates investigated. A *P*-value of < 0.05 was considered to be statistically significant. All statistical analyses were performed using JMP version 10.1 software (SAS Institute, Inc., Cary, NC, USA), SPSS version 22 software (Japan IBM, Tokyo, Japan) and R version 3.3.1 (http://www.r-project.org).

Results

One-hundred-and-eighteen eyes of 89 participants were initially enrolled. Eighteen eyes were excluded from study with poor quality OCT-A images (13), poor fixation (2), motion artifact (2), and fovea off center (1). There then were 100 eyes (32 glaucoma eyes of 26 patients, 30 glaucoma suspect eyes of 22 patients, and 38 healthy eyes of 29 subjects) available for analysis. Table 1 summarizes the baseline characteristics of the study subjects. The median number of examinations was 3 (2 for 28 eyes, 3 for 42 eyes, 4 for 16 eyes and 5 or more for 14 eyes). The patients were followed over a mean period of 13.1 (glaucoma group) to 13.9 months (glaucoma suspect group). The follow-up period, number of visits, axial length, and central corneal thickness were not significantly different among diagnostic groups. There were also no statistically significant differences between systolic BP, diastolic BP, mean BP, and mean ocular perfusion pressure measurements among groups. Topical medications were unchanged during the follow up (except for one patient that had a topical beta blocker added). The visual field mean deviation (MD) and PSD were significantly worse in glaucoma eyes compared to healthy and glaucoma suspect eyes (P < 0.001). Baseline macula vessel density was highest in normal eyes followed by glaucoma suspect and glaucoma eyes for the whole (52.3%, 48.9%, and 47.8%, respectively), superior (53.0%, 50.1%, and 48.5%, respectively), and inferior en-face regions (52.6%, 49.7%, and 48.2%, respectively) (P < 0.001 for all).

Figure 2, as an example, shows the change in vessel density maps over time in a healthy subject and a glaucoma patient. The healthy eye has a denser capillary network in the macula region which remained stable over time. In contrast, the glaucoma eye tended to have a sparser microvascular network, which decreased over time regardless of SSI values, whereas both cpRNFL and GCC thickness using SD-OCT analysis were unchanged over time.

Quantitative Assessment of Change Over Time

The rate of change in vessel density (%/year) was significantly different among the groups (P < 0.05 for all) (Figure 3). Table 2 shows values of mean rates of change of vessel density over time for each sector. The mean rate of macula vessel density loss was significantly different from zero, both globally and by sector, only in glaucoma eyes. (P < 0.05 for all).

The mean rate of macula vessel density loss was not significantly different from zero in healthy and glaucoma suspect eyes.

The mean rate of change in macula whole en-face vessel density was significantly faster in glaucoma eyes (−2.23 %/yr) than in glaucoma suspect (0.87%/yr, P = 0.001) and healthy eyes (0.29 %/yr, P = 0.004). In both superior and inferior sectors, the mean rate of vessel density loss was significantly faster in glaucoma eyes compared with healthy and glaucoma suspect eyes (all P < 0.05). In contrast to vessel density measurements, the rate of change in GCC thickness was not significantly different from zero in any of the diagnostic groups and the rate of GCC thinning was not significantly faster in glaucoma eyes compared to glaucoma suspect and healthy eyes (Table 2).

Based on the univariate analysis (Supplemental Table), age, diastolic blood pressure, mean ocular perfusion pressure, and SSI were significantly associated with vessel density change and were therefore included in the multivariable analysis. In multivariate analysis, the mean rate of change in macula whole en-face vessel density was significantly faster in glaucoma eyes than in glaucoma suspect (mean difference in rates −2.30 %/year; P = 0.001) and healthy eyes (mean difference in rates −2.13 %/year; P = 0.009) (Table 3). Glaucoma eyes also tended to have a significantly faster rate of macula vessel density dropout than glaucoma suspect and healthy eyes in both the superior region (mean difference in rates −2.24 %/year; P = 0.004 and mean difference in rates −2.23 %/year; P = 0.033, respectively) and the inferior region (mean difference in rates −2.86 %/year; P = 0.001 and mean difference in rates −3.77 %/year; P < 0.001, respectively). In addition, the rate of vessel density change in glaucoma eyes was significantly faster than in healthy and glaucoma suspect eyes in the other sectors.

Discussion

Even with a relatively short follow-up of 13 months, this study demonstrated that rate of macula vessel density loss in glaucoma eyes was significantly faster than both glaucoma suspect and healthy eyes. In contrast, the rate of change in GCC thickness was not significantly different from zero, and no significant differences in the rate of GCC change among diagnostic groups were found.

Gadde et al. used local fractal analysis to calculate macula vessel densities within a 2.5 mm diameter circle in normal eyes and reported mean (±standard error) values of 53.62 (±3.46) %[36]. Toto reported 50.4% as the mean parafoveal vessel density in healthy eyes. [37] These results were comparable to the results of the healthy eyes in our study. Additionally, in the current study, although the baseline vessel density was significantly lower in both glaucoma and glaucoma-suspect eyes than in healthy eyes and similar between glaucoma suspects and glaucoma eyes, the rate of change was significantly faster in the glaucoma eyes compared to healthy and glaucoma suspect eyes. In the current study, vessel density changes correlated to a previous longitudinal analysis of macula full thickness using SD-OCT[38]. In that study, there were significantly faster mean rates of change in average macula thickness in the progression group compared to the stable disease group, though the baseline macula thickness was similar in the two groups. Interestingly, even though the rate of change in

GCC thickness was not significantly different from zero in any of the groups, loss of vessel density in the glaucoma group was significantly faster. Although the reason for this is unclear, it is possible that it may be related to the "dynamic range" being different between neural structural changes and vessel density changes. In this regard, neural tissue may decrease earlier in the glaucoma continuum than vessel density. As the glaucoma patients in this study predominantly were individuals with moderate severity (median MD; −6.9 dB), the vessel density changes may be detected first in these patients. Alternatively, vessel density changes may just be occurring earlier regardless of the stage of the disease. Additional follow-up in larger numbers of patients with various stages of disease is needed to clarify these results.

Our results are discrepant with those of Rao et al.[27] They reported that the diagnostic ability of the vessel density parameters of OCT-A was only moderate and macula vessel density had significantly lower diagnostic abilities in POAG than the peripapillary density. However, their glaucoma group consisted predominantly of individuals with pre-perimetric and early stage disease, which may account for the relatively low diagnostic accuracy of macula vessel density measurements for distinguishing between healthy and glaucoma eyes.

It previously has been hypothesized that evaluation of OCT-A vessel density can improve our ability to manage glaucoma.[20] Because RGCs are so metabolically active [23] and depend on regional capillary networks to meet their tremendous metabolic requirements, assessment of retinal vasculature in the macula region may also improve our ability to detect glaucomatous changes. The faster rate of vessel density loss in glaucoma eyes could reflect the existence of dysfunctional or senescent RGCs that have lower metabolic demands.

Age and SSI were also significantly associated with baseline vessel density measurements. Recent studies have shown conflicting results about the effect of age on the macula vessel density measurements. Gadde et al. reported that age did not affect SCP vessel density,[36] while other reports found that SCP vessel density decreased with increasing age.[19, 31, 39, 40] The study by Gadde et al. had a relatively small sample size (n = 18) and a younger (< 68 years) age group, which may explain at least in part the differences in the results. Additionally, the impact of SSI on the vessel density measurements was significant and strong (coefficient: 0.29% to 0.37% per unit in multivariate analysis) in this study. SSI has been shown to affect quantitative OCT measurement and is determined by patient-related factors, such as ocular media. It also may be affected by operator-related factors, such as alignment of the scan and the scan beam focus.[41] Our results support the hypothesis by Shahlaee[19] that macula density values may need to be corrected for age and signal strength when used for clinical assessment. For this reason, we only included images that passed review by trained graders, and both SSI and age were accounted for in the multivariable analyses using mixed effects model.

Further, IOP was not correlated with vessel density in this study. This result is consistent with the hypothesis of Rao et al.[27] that the lower macula vessel density in glaucoma eyes might be independent of the IOP levels at which glaucoma develops, or it could be because the IOP of glaucoma patients was lowered. Although IOP was checked every 6 months in

the current study, more measurements and longer follow up would be needed to more clearly elucidate this relationship.

The results of the present study suggest that even in a relatively brief follow-up period, OCT-A is able to detect longitudinal reduction of macula vessel density in glaucoma eyes. However, it should be noted that vascular measurements obtained by this technology only reflect some aspects of blood flow within the detected vessels, and does not represent an estimate of real blood flow. Specifically, this modality detects vasculature based on amplitude decorrelation, which results from perfused vessels, but does not directly quantify the flow rate within the detected vessels. Therefore, the reduced vessel density that we observed could be the result of either capillary dropout or very slow rates of blood flow within the perfused vasculature.

Some limitations of this investigation warrant discussion. First, even though the rate of decrease in the vessel density in this longitudinal study using OCT-A was significantly different among the groups, the follow-up period was relatively short. OCT-A was introduced recently, and longer follow-up is ongoing. Second, although this was not directly studied in the current study, the repeatability of superficial macular vessel density measurements in glaucoma eyes has been reported recently to be similar in healthy and mild to moderate glaucoma eyes in another group of patients. [42] Moreover, we have found in a separate cohort of our patients that intra-visit and inter-visit reproducibility of superficial macula vessel density was good in both glaucoma and healthy eyes, but worse than their reproducibility for GCC. (Weinreb RN, written communication, June 20, 2017). These results also are comparable to other reports of estimates of the reproducibility of vessel density measurements[15, 18, 19, 42, 43] and measures of GCC. [44, 45] As the reproducibility of macula vessel density is worse than with GCC, one would expect the likelihood of detecting significant change of vessel density to be lower than detection of GCC change. Therefore, these reproducibility values cannot explain why the rate of macula vessel density change over time, and not GCC, was significant. Another limitation of this study was the relatively small sample size, which limited the power for evaluating the effect of some possible confounding variables on the rate of decrease in vessel density. In our results, some glaucomatous eyes show faster dropout, while other eyes seem to be stable (Figure 3). The significance of these differences is not known. Larger longitudinal studies are needed to investigate whether faster rates of macula vessel density loss in glaucoma eyes are associated with the severity of glaucomatous structural and functional progression, and whether macula vessel density loss may even be predictive of such progression.

In conclusion, after less than 14 months follow-up, eyes with POAG had significantly faster loss of OCT-A macula vessel density than either glaucoma suspect or healthy eyes. Serial OCT-A measurements also detected glaucomatous change in macula vessel density in eyes without evidence of change in GCC thickness. OCT-A can monitor microvascular changes in glaucoma, and also may improve our understanding of the pathophysiology of the disease.

Supplementary Material

Refer to Web version on PubMed Central for supplementary material.

Acknowledgments

References

1. Weinreb RN, Khaw PT. Primary open-angle glaucoma. Lancet. 2004; 363(9422):1711–1720. [PubMed: 15158634]

2. Weinreb, RN., Harris, A. Ocular blood flow in glaucoma. Amsterdam, The Netherlands: Kugler Publications; 2009.

3. Flammer J, Orgul S, Costa VP, et al. The impact of ocular blood flow in glaucoma. Prog Retin Eye Res. 2002; 21(4):359–393. [PubMed: 12150988]

4. Grieshaber MC, Mozaffarieh M, Flammer J. What is the link between vascular dysregulation and glaucoma? Surv Ophthalmol. 2007; 52(Suppl 2):S144–154. [PubMed: 17998040]

5. Harris A, Rechtman E, Siesky B, Jonescu-Cuypers C, McCranor L, Garzozi HJ. The role of optic nerve blood flow in the pathogenesis of glaucoma. Ophthalmol Clin North Am. 2005; 18(3):345–353. [PubMed: 16054992]

6. Mansouri K. Optical coherence tomography angiography and glaucoma: searching for the missing link. Expert Rev Med Devices. 2016; 13(10):879–880. [PubMed: 27580072]

7. Plange N, Kaup M, Weber A, Remky A, Arend O. Fluorescein filling defects and quantitative morphologic analysis of the optic nerve head in glaucoma. Arch Ophthalmol. 2004; 122(2):195–201. [PubMed: 14769596]

8. O'Brart DP, de Souza Lima M, Bartsch DU, Freeman W, Weinreb RN. Indocyanine green angiography of the peripapillary region in glaucomatous eyes by confocal scanning laser ophthalmoscopy. Am J Ophthalmol. 1997; 123(5):657–666. [PubMed: 9152071]

9. Rechtman E, Harris A, Kumar R, et al. An update on retinal circulation assessment technologies. Curr Eye Res. 2003; 27(6):329–343. [PubMed: 14704917]

10. Nicolela MT, Hnik P, Drance SM. Scanning laser Doppler flowmeter study of retinal and optic disk blood flow in glaucomatous patients. Am J Ophthalmol. 1996; 122(6):775–783. [PubMed: 8956631]

11. Michelson G, Schmauss B, Langhans MJ, Harazny J, Groh MJ. Principle, validity, and reliability of scanning laser Doppler flowmetry. J Glaucoma. 1996; 5(2):99–105. [PubMed: 8795741]

12. Petrig BL, Riva CE, Hayreh SS. Laser Doppler flowmetry and optic nerve head blood flow. Am J Ophthalmol. 1999; 127(4):413–425. [PubMed: 10218694]

13. Yaoeda K, Shirakashi M, Funaki S, Funaki H, Nakatsue T, Abe H. Measurement of microcirculation in the optic nerve head by laser speckle flowgraphy and scanning laser Doppler flowmetry. Am J Ophthalmol. 2000; 129(6):734–739. [PubMed: 10926981]

14. Jia Y, Bailey ST, Hwang TS, et al. Quantitative optical coherence tomography angiography of vascular abnormalities in the living human eye. Proc Natl Acad Sci U S A. 2015; 112(18):E2395–2402. [PubMed: 25897021]

15. Jia Y, Wei E, Wang X, et al. Optical coherence tomography angiography of optic disc perfusion in glaucoma. Ophthalmology. 2014; 121(7):1322–1332. [PubMed: 24629312]

16. Spaide RF, Klancnik JM Jr, Cooney MJ. Retinal vascular layers imaged by fluorescein angiography and optical coherence tomography angiography. JAMA Ophthalmol. 2015; 133(1):45–50. [PubMed: 25317632]

17. Jia Y, Tan O, Tokayer J, et al. Split-spectrum amplitude-decorrelation angiography with optical coherence tomography. Opt Express. 2012; 20(4):4710–4725. [PubMed: 22418228]

18. Liu L, Jia Y, Takusagawa HL, et al. Optical Coherence Tomography Angiography of the Peripapillary Retina in Glaucoma. JAMA Ophthalmol. 2015; 133(9):1045–1052. [PubMed: 26203793]

19. Shahlaee A, Samara WA, Hsu J, et al. In Vivo Assessment of Macular Vascular Density in Healthy Human Eyes Using Optical Coherence Tomography Angiography. Am J Ophthalmol. 2016; 165:39–46. [PubMed: 26921803]

20. Yarmohammadi A, Zangwill LM, Diniz-Filho A, et al. Optical Coherence Tomography Angiography Vessel Density in Healthy, Glaucoma Suspect, and Glaucoma Eyes. Invest Ophthalmol Vis Sci. 2016 Oct; 57(9):451–459.

21. Akagi T, Iida Y, Nakanishi H, et al. Microvascular Density in Glaucomatous Eyes With Hemifield Visual Field Defects: An Optical Coherence Tomography Angiography Study. Am J Ophthalmol. 2016; 168:237–249. [PubMed: 27296492]

22. Yarmohammadi A, Zangwill LM, Diniz-Filho A, et al. Relationship between Optical Coherence Tomography Angiography Vessel Density and Severity of Visual Field Loss in Glaucoma. Ophthalmology. 2016; 123(12):2498–2508. [PubMed: 27726964]

23. Yu DY, Cringle SJ, Balaratnasingam C, Morgan WH, Yu PK, Su EN. Retinal ganglion cells: Energetics, compartmentation, axonal transport, cytoskeletons and vulnerability. Prog Retin Eye Res. 2013; 36:217–246. [PubMed: 23891817]

24. Yu DY, Yu PK, Cringle SJ, Kang MH, Su EN. Functional and morphological characteristics of the retinal and choroidal vasculature. Prog Retin Eye Res. 2014; 40:53–93. [PubMed: 24583621]

25. Garway-Heath DF, Caprioli J, Fitzke FW, Hitchings RA. Scaling the hill of vision: the physiological relationship between light sensitivity and ganglion cell numbers. Invest Ophthalmol Vis Sci. 2000; 41(7):1774–1782. [PubMed: 10845598]

26. Curcio CA, Allen KA. Topography of ganglion cells in human retina. J Comp Neurol. 1990; 300(1):5–25. [PubMed: 2229487]

27. Rao HL, Pradhan ZS, Weinreb RN, et al. Regional Comparisons of Optical Coherence Tomography Angiography Vessel Density in Primary Open-Angle Glaucoma. Am J Ophthalmol. 2016; 171:75–83. [PubMed: 27590118]

28. Sample PA, Girkin CA, Zangwill LM, et al. The African Descent and Glaucoma Evaluation Study (ADAGES): design and baseline data. Arch Ophthalmol. 2009; 127(9):1136–1145. [PubMed: 19752422]

29. Jia Y, Morrison JC, Tokayer J, et al. Quantitative OCT angiography of optic nerve head blood flow. Biomed Opt Express. 2012; 3(12):3127–3137. [PubMed: 23243564]

30. Spaide RF, Fujimoto JG, Waheed NK. Optical Coherence Tomography Angiography. Retina. 2015; 35(11):2161–2162. [PubMed: 26502006]

31. Yu J, Jiang C, Wang X, et al. Macular perfusion in healthy Chinese: an optical coherence tomography angiogram study. Invest Ophthalmol Vis Sci. 2015; 56(5):3212–3217. [PubMed: 26024105]

32. Racette L, Liebmann JM, Girkin CA, et al. African Descent and Glaucoma Evaluation Study (ADAGES): III. Ancestry differences in visual function in healthy eyes. Arch Ophthalmol. 2010; 128(5):551–559. [PubMed: 20457975]

33. Tan O, Chopra V, Lu AT, et al. Detection of macular ganglion cell loss in glaucoma by Fourier-domain optical coherence tomography. Ophthalmology. 2009; 116(12):2305–2314. e2301–2302. [PubMed: 19744726]

34. Alencar LM, Zangwill LM, Weinreb RN, et al. A comparison of rates of change in neuroretinal rim area and retinal nerve fiber layer thickness in progressive glaucoma. Invest Ophthalmol Vis Sci. 2010; 51(7):3531–3539. [PubMed: 20207973]

35. Medeiros FA, Alencar LM, Zangwill LM, et al. Detection of progressive retinal nerve fiber layer loss in glaucoma using scanning laser polarimetry with variable corneal compensation. Invest Ophthalmol Vis Sci. 2009; 50(4):1675–1681. [PubMed: 19029038]

36. Gadde SG, Anegondi N, Bhanushali D, et al. Quantification of Vessel Density in Retinal Optical Coherence Tomography Angiography Images Using Local Fractal Dimension. Invest Ophthalmol Vis Sci. 2016; 57(1):246–252. [PubMed: 26803800]

37. Toto L, Borrelli E, Mastropasqua R, et al. Association between outer retinal alterations and microvascular changes in intermediate stage age-related macular degeneration: an optical coherence tomography angiography study. Br J Ophthalmol. 2017; 101(6):774–779. [PubMed: 27625163]

38. Sung KR, Sun JH, Na JH, Lee JY, Lee Y. Progression detection capability of macular thickness in advanced glaucomatous eyes. Ophthalmology. 2012; 119(2):308–313. [PubMed: 22182800]

39. Iafe NA, Phasukkijwatana N, Chen X, Sarraf D. Retinal Capillary Density and Foveal Avascular Zone Area Are Age-Dependent: Quantitative Analysis Using Optical Coherence Tomography Angiography. Invest Ophthalmol Vis Sci. 2016; 57(13):5780–5787. [PubMed: 27792812]

40. Coscas F, Sellam A, Glacet-Bernard A, et al. Normative Data for Vascular Density in Superficial and Deep Capillary Plexuses of Healthy Adults Assessed by Optical Coherence Tomography Angiography. Invest Ophthalmol Vis Sci. 2016 Oct; 57(9):211–223.

41. Vizzeri G, Bowd C, Medeiros FA, Weinreb RN, Zangwill LM. Effect of signal strength and improper alignment on the variability of stratus optical coherence tomography retinal nerve fiber layer thickness measurements. Am J Ophthalmol. 2009; 148(2):249–255. e241. [PubMed: 19427621]

42. Venugopal JP, Rao HL, Weinreb RN, et al. Repeatability of vessel density measurements of optical coherence tomography angiography in normal and glaucoma eyes. Br J Ophthalmol. 2017 in press.

43. Dong J, Jia YD, Wu Q, et al. Interchangeability and reliability of macular perfusion parameter measurements using optical coherence tomography angiography. Br J Ophthalmol. 2017 in press.

44. Wolf-Schnurrbusch UE, Ceklic L, Brinkmann CK, et al. Macular thickness measurements in healthy eyes using six different optical coherence tomography instruments. Invest Ophthalmol Vis Sci. 2009; 50(7):3432–3437. [PubMed: 19234346]

45. Garas A, Vargha P, Hollo G. Reproducibility of retinal nerve fiber layer and macular thickness measurement with the RTVue-100 optical coherence tomograph. Ophthalmology. 2010; 117(4):738–746. [PubMed: 20079538]

Biography

Takuhei Shoji, MD, PhD, is an international research fellow at the Hamilton Glaucoma Center, Shiley Eye Institute, University of California at San Diego, California. He completed his residency in ophthalmology at National Defense Medical College, Japan and DrPH degree at the Graduate School of Medicine, Keio University, Japan. His research interests clinical ophthalmology, imaging in glaucoma, epidemiology, and surgical innovations in glaucoma.
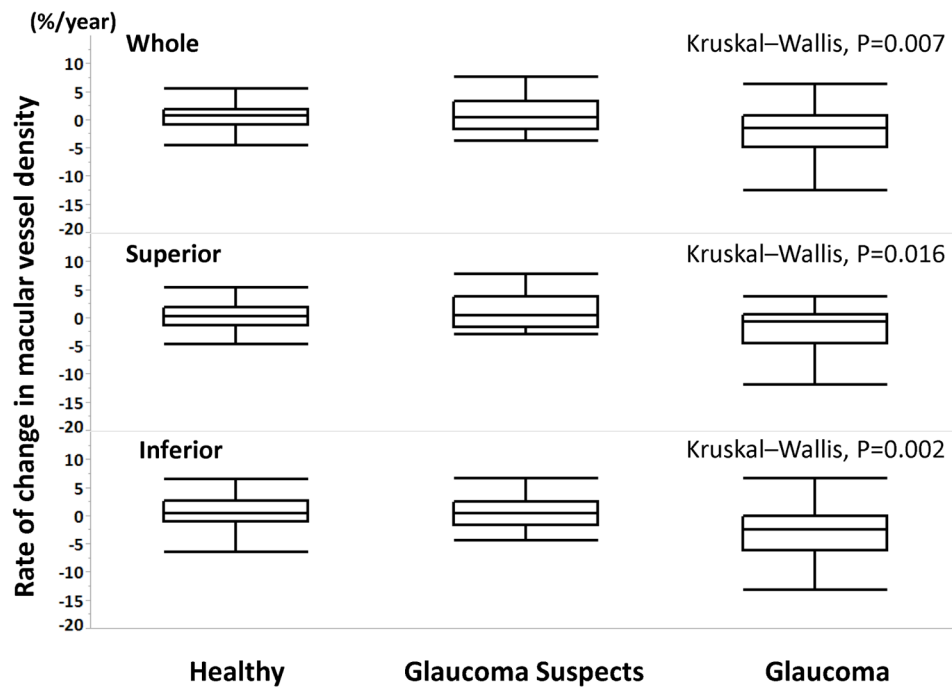
Figure 1.

A spectral domain optical coherence tomography angiography (OCT-A) 3 × 3 scan of the macula showing the superficial vascular plexus. The AngioVue software automatically defined a 3.0 mm × 3.0 mm square area as the whole en-face region (A), which was divided into 2 regions (white dotted line) into the superior and inferior en-face area. Moreover, a central (inner pink) circle was defined as the fovea (B), and the parafoveal region was defined as a ring surrounding the foveal region (C–F). The parafoveal region was also divided into 4 sectors of 90°, viz., as para-temporal (C), superior (D), nasal (E), and inferior (F).
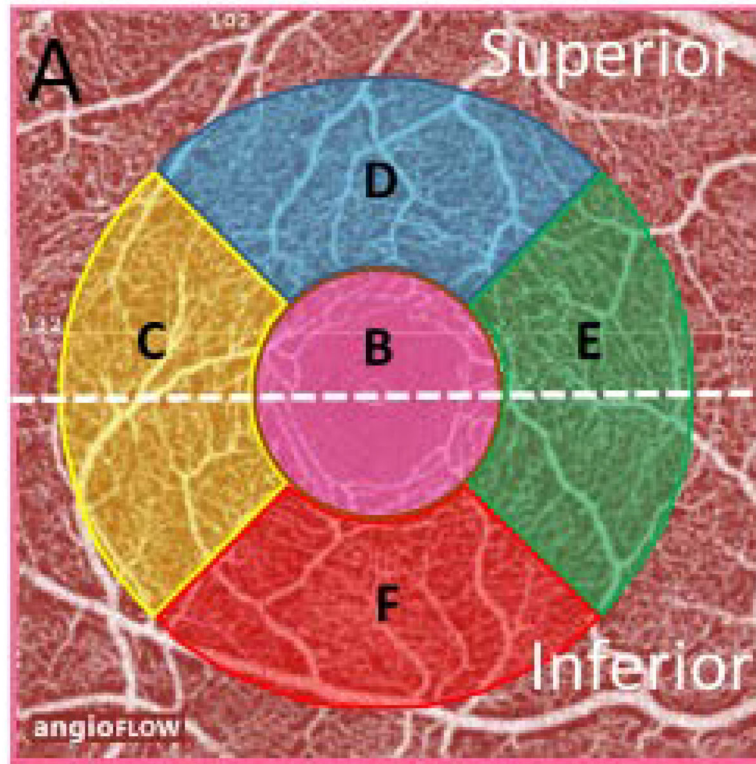
Figure 2.
Longitudinal changes in optical coherence tomography angiography images of the superficial retinal vascular plexus (3.0 mm × 3.0 mm scan size) in a healthy and in a glaucomatous eye. Top and fifth row: fundus photograph (left) and vessel density map, seen over time in healthy subject using optical coherence tomography (OCT) -angiography(A). Second and sixth row: standard automated perimetry (SAP) results (left) and area density color-coded map in a healthy subject (2nd row) and glaucoma patients (6th row). OCT-A macula scan showing the superficial vascular plexus; corresponding color-coded flow density map of the superficial vascular plexus flow density (the warmer the color, the greater the flow). This healthy case shows vessel density was almost unchanged (56.23% to 57.38%) over time. In contrast, vessel density was decreased 50.06% to 44.38% overtime, regardless of SSI in glaucoma patients. Third and seventh row: ganglion cell complex (GCC) map over time. The measurement parameters from GCC thickness of analysis are automatically compared to the OCT's normative limits, and the results are color-coded for "within normal limits" (green), "borderline" (yellow), and "outside normal limits" (red). The average GCC thickness was also almost unchanged over time both healthy subjects (104.7μm to 105.5μm) and glaucoma patients (59.4μm to 60.5μm). Fourth and bottom row: optic nerve head (ONH) thickness color-coded map (the warmer the color, the greater the thickness) and results of sector analysis automatically compared to the OCT's normative limits, color-coded for "within normal limits" (green), "borderline" (yellow), and "outside normal limits" (red) at outer ring. The average cpRNFL thickness was also almost unchanged over time in both cases.
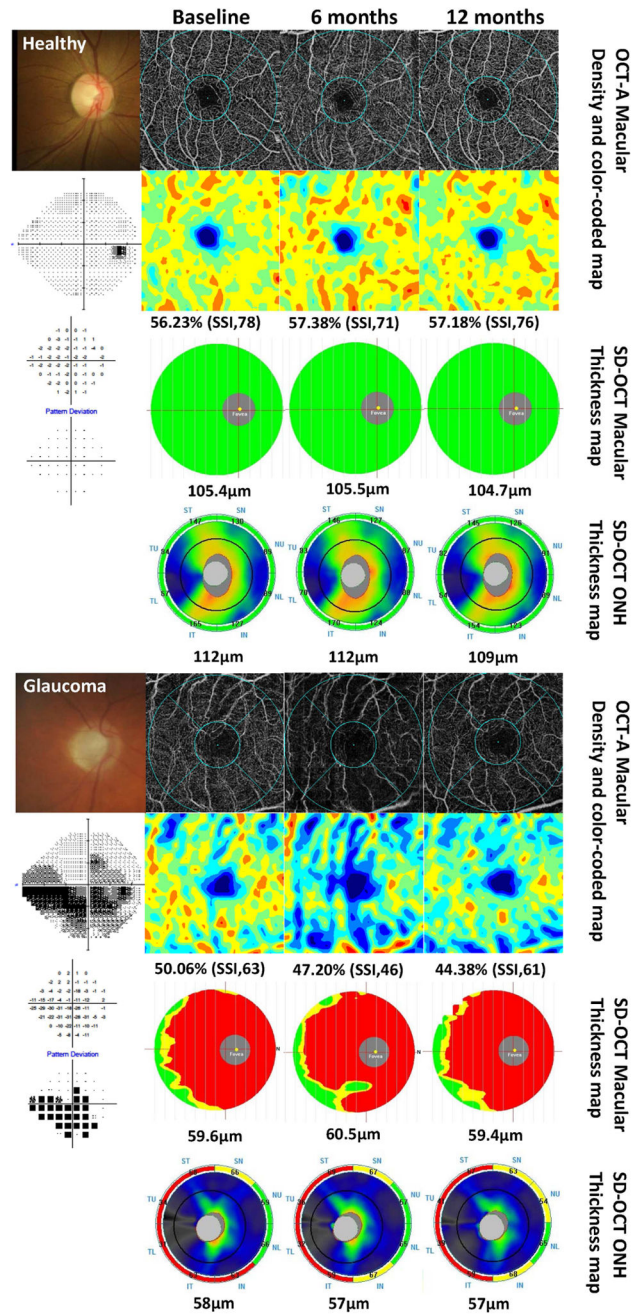
Figure 3.
Boxplots illustrating the distribution of the rate of vessel density change (%/year) in whole en-face vessel density (top), superior en-face vessel density (middle), and inferior en-face vessel density (bottom) measurements in healthy, glaucoma-suspects, and glaucomatous eyes. The medians are represented by horizontal lines in the white boxes. Boxes represent the interquartile range (IQR) between the first and third quartiles.

Table 1

Demographics and Ocular Characteristics of Study Population

Variables	A. Healthy (n = 38)	B. Glaucoma Suspect (n = 30)	C. Glaucoma (n = 32)	P value	Post Hoc Significance
Age (yrs.)	70.7 ± 13.1	70.0 ± 7.0	71.8 ± 9.7	0.715*	
Gender (male/female)	17/21	9/21	19/13	0.067	
Follow up period (mo.)	13.7 ± 1.8	13.9 ± 1.9	13.1 ± 1.6	0.233	
Number of visits (median[25,75 percentile])	3 (2, 4)	3 (2, 4)	3 (3,4)	0.055†	
Clinical characteristics					
Blood Pressure (mmHg)					
Systolic	132.2 ± 15.9	133.4 ± 20.7	128.6 ± 16.7	0.533*	
Diastolic	77.2 ± 9.7	79.1 ± 10.3	74.6 ± 8.8	0.191*	
Mean	95.3 ± 10.2	97.0 ± 12.9	92.4 ± 10.7	0.269*	
MOPP, mm Hg	49.3 ± 7.9	47.6 ± 10.7	47.3 ± 7.7	0.560*	
Heart rate (beats/min)	66.3 ± 12.0	67.9 ± 16.3	65.5 ± 11.3	0.770*	
Self-reported history of diabetes, n (%)	2 (5.3)	0 (0)	3 (9.4)	0.238	
Self-reported history of hypertension, n (%)	8 (21.1)	8 (26.7)	5 (15.6)	0.566	
Diabetes medications, n (%)	0 (0)	0 (0)	2 (6.3)	0.114	
Antihypertensive medications, n (%)	6 (15.8)	4 (13.3)	3 (9.4)	0.728	
Topical glaucoma medications, n (%)	0 (0)	23 (76.7)	27 (84.4)	**<0.001**	A < B =C
Ocular characteristics					
MD (dB) (median[25,75 percentile])	−0.6 (−2.2, 0.5)	−0.8 (−1.7, −0.1)	−6.9 (−11.3, −4.2)	**<0.001†**	A = B >C
PSD (dB) (median[25,75 percentile])	1.7 (1.4, 2.4)	1.7 (1.5, 2.2)	8.9 (4.2, 11.5)	**0.001†**	A = B < C
Axial Length (mm)	24.1 ± 1.1	24.1 ± 1.5	24.5± 1.3	0.324*	
CCT (μm)	543.8± 35.4	555.0± 44.5	539.3± 44.9	0.334*	
Average GCC (μm)	91.0 ± 9.2	87.5 ± 10.4	74.0 ± 11.7	**<0.001***	A = B >C
Superior GCC (μm)	91.0 ± 9.1	88.0 ± 10.4	76.5 ± 13.2	**<0.001***	A = B >C
Inferior GCC (μm)	91.0 ±10.0	87.0 ±11.1	71.6 ±13.0	**<0.001***	A = B >C
GLV	7.0 ± 7.0	10.0 ± 6.9	22.6 ± 9.7	**<0.001***	A = B < C
FLV	1.8 ± 3.0	1.8 ± 1.8	7.0 ± 7.2	**<0.001***	A = B < C

Variables	A. Healthy (n = 38)	B. Glaucoma Suspect (n = 30)	C. Glaucoma (n = 32)	P value	Post Hoc Significance
Baseline Vessel Density (%)					
Whole-en-face	52.3 ± 3.1	48.9 ± 4.5	47.8 ± 4.4	**<0.001***	A > B =C
Superior-en-face	53.0 ± 3.4	50.1± 4.5	48.5 ± 4.9	**0.002***	A > B =C
Inferior-en-face	52.6 ± 3.8	49.7 ± 5.6	48.2 ± 5.0	**0.009***	A > B =C
Baseline SSI	65.8 ± 10.9	63.4 ± 8.3	61.5 ± 5.5	0.112	

Abbreviations: yrs, years; mo, months: MOPP, mean ocular perfusion pressure: MD, mean deviation; dB, decibels; PSD, pattern standard deviation; CCT, central corneal thickness: GCC, ganglion cell complex: SSI, signal strength index

Categorical variables were compared using the chi-square test.

Data expressed as mean ± standard deviation were compared with ANOVA.

Post hoc significance was using Tukey's honest significant difference test.

Data expressed as the median (25,75 percentile) were compared using the nonparametric Kruskal–Wallis test. Post hoc significance was using Dunnet multiple comparisons.

Values with statistical significance are shown in bold.

Table 2

Summary Table of Mean Thickness and Vessel Density Slope Values in Healthy, Glaucoma Suspect and Glaucoma Eyes

The rate of change (per year)	Healthy		Glaucoma Suspect		Glaucoma		Difference between Healthy and Glaucoma		Difference between Glaucoma suspect and Glaucoma	
	Mean (95%CI)	P Value*	Mean (95%CI)	P Value*	Mean (95%CI)	P Value*	Mean (95%CI)	P Value†	Mean (95%CI)	P Value†
OCT (Thickness, μm/year)										
Ganglion Cell Complex	−0.92 (−2.15, 0.32)	0.148	−0.10 (1.57, 1.38)	0.899	−0.44 (−1.57, 1.38)	0.532	−0.48 (−2.32, 1.35)	0.609	−0.34 (−2.34, 1.66)	0.740
OCT-A (Vessel Density, %/year)										
Whole-en-face	0.29 (−0.82, 1.40)	0.610	0.87 (−0.47, 2.22)	0.204	−2.23 (−3.52, −0.93)	**<0.001**	−2.52 (−0.80, −2.86)	**0.004**	−3.10 (−4.96, −1.24)	**0.001**
Superior-en-face	−0.00 (−1.11, 1.11)	0.998	1.04 (−0.30, 2.38)	0.129	−1.97 (−3.28, −0.67)	**0.003**	−1.97 (−0.25, −3.68)	**0.025**	−3.01 (−4.88, −1.15)	**0.002**
Inferior-en-face	0.50 (−0.76, 1.75)	0.441	0.74 (−0.77, 2.26)	0.341	−2.90 (−4.37, −1.44)	**<0.001**	−3.40 (−5.32, −1.48)	**<0.001**	−3.65 (−5.73, −1.56)	**<0.001**
Para Fovea	0.53 (−0.83, 1.89)	0.444	0.89 (−0.75, 2.52)	0.292	−3.13 (−4.70, −1.56)	**<0.001**	−3.66 (−5.73, −1.58)	**<0.001**	−4.01 (−6.27, −1.75)	**<0.001**
Para-Temporal	0.48 (−0.82, 1.79)	0.471	0.75 (−0.77, 2.38)	0.319	−1.81 (−0.29, −3.32)	**0.021**	−2.29 (−4.29, −0.29)	**0.026**	−2.61 (−4.79, −0.43)	**0.020**
Para-Superior	0.36 (−1.00, 1.73)	0.603	0.48 (−0.91, 2.40)	0.378	−2.00 (−3.58, −0.43)	**0.015**	−2.37 (−4.45, −0.29)	**0.028**	−2.75 (−5.01, −0.49)	**0.019**
Para-Nasal	0.30 (−1.14, 1.74)	0.686	0.74 (−1.00, 2.48)	0.407	−3.34 (−5.01, −1.67)	**<0.001**	−3.64 (−5.84, −1.43)	**0.002**	−4.08 (−6.48, −1.68)	**0.001**
Para-Inferior	0.77 (−0.69, 2.23)	0.303	0.59 (−1.18, 2.35)	0.517	−2.73 (−4.42, −1.04)	**0.002**	−3.51 (−5.74, −1.27)	**0.003**	−3.32 (−5.75, −0.88)	**0.009**

*
p-value representing whether the mean rate of change is significantly different from zero

†
p-value based on post-hoc ANOVA testing using the Tukey's honest significant difference test

Values with statistical significance are shown in bold.

Abbreviations: CI, confidence interval; OCT, optical coherence tomography; GCC, ganglion cell complex; OCT-A, optical coherence tomography angiography

Table 3

Association Between Vessel Density and Demographic and Ocular Variables: Multivariable Analysis*

	Vessel Density (%)							
	Whole		Superior		Inferior		ParaFovea	
Variables	Coefficients (95%CI)	P Value	Coefficients (95%CI)	P Value	Coefficients (95%CI)	P Value	Coefficients (95%CI)	P Value
Age (per y.)	−0.08 (−0.17, 0.01)	0.086	−0.13 (−0.27, 0.02)	0.084	−0.09 (−0.25, 0.06)	0.230	−0.08 (−0.18, 0.01)	0.085
Glaucoma (reference: Glaucoma)								
Healthy	1.02 (−1.18, 3.21)	0.364	0.85 (−2.44, 4.14)	0.611	−0.16 (−3.28, 2.96)	0.919	0.42 (−2.01, 2.84)	0.738
Glaucoma Suspect	1.07 (−1.09, 3.24)	0.331	1.56 (−0.95, 4.08)	0.222	1.46 (−1.07, 3.99)	0.258	0.73 (−1.64, 3.10)	0.548
Time (per y.)	−1.99 (−3.18, −0.81)	**0.001**	−1.64 (−3, −0.27)	**0.019**	−2.86 (−4.17, −1.54)	**<0.001**	−2.99 (−4.67, −1.33)	**0.001**
Diastolic Blood Pressure (per mmHg)	0.00 (−0.14, 0.15)	0.959	−0.01 (−0.19, 0.16)	0.882	0.02 (−0.18, 0.21)	0.871	0.02 (−0.12, 0.16)	0.814
MOPP (per mmHg)	0.07 (−0.06, 0.20)	0.315	0.07 (−0.08, 0.23)	0.355	0.04 (−0.14, 0.22)	0.687	0.09 (−0.04, 0.21)	0.170
SSI (per unit)	0.25 (0.16, 0.34)	**<0.001**	0.22 (0.12, 0.32)	**<0.001**	0.28 (0.17, 0.40)	**<0.001**	0.28 (0.18, 0.38)	**<0.001**
Time x glaucoma (reference: Glaucoma)(per y.)								
Healthy	2.13 (0.53, 3.74)	**0.009**	2.23 (0.19, 4.28)	**0.033**	3.77 (1.92, 5.62)	**<0.001**	3.33 (1.24, 5.41)	**0.002**
Glaucoma Suspect	2.30 (0.99, 3.60)	**0.001**	2.24 (0.71, 3.76)	**0.004**	2.86 (1.13, 4.60)	**0.001**	3.11 (1.19, 5.02)	**0.001**

	Para-Temporal		Para-Superior		Para-Nasal		Para-Inferior	
Variables	Coefficients (95%CI)	P Value	Coefficients (95%CI)	P Value	Coefficients (95%CI)	P Value	Coefficients (95%CI)	P Value
Age (per y.)	−0.07 (−0.17, 0.03)	0.191	−0.11 (−0.2, −0.01)	**0.024**	−0.09 (−0.19, 0.01)	0.071	−0.06 (−0.17, 0.05)	0.286
Glaucoma (reference: Glaucoma)								
Healthy	0.58 (−1.99, 3.16)	0.657	1.62 (−0.92, 4.16)	0.212	−0.37 (−2.84, 2.1)	0.770	0.74 (−1.8, 3.27)	0.568
Glaucoma Suspect	1.21 (−1.12, 3.54)	0.309	1.27 (−1.28, 3.82)	0.329	−0.02 (−2.57, 2.53)	0.988	1.72 (−0.85, 4.28)	0.189
Time (per y.)	−1.62 (−3.12, −0.13)	**0.033**	−1.49 (−3.29, 0.32)	0.106	−3.02 (−4.62, −1.43)	**<0.001**	−2.58 (−4.05, −1.10)	**0.001**
Diastolic Blood Pressure (per mmHg)	−0.03 (−0.18, 0.12)	0.715	0.05 (−0.09, 0.20)	0.448	0.01 (−0.14, 0.16)	0.945	0.04 (−0.13, 0.21)	0.646
MOPP (per mmHg)	0.11 (−0.04, 0.27)	0.154	0.03 (−0.09, 0.15)	0.627	0.08 (−0.04, 0.20)	0.199	0.08 (−0.08, 0.25)	0.330
SSI (per unit)	0.25 (0.14, 0.35)	**<0.001**	0.25 (0.15, 0.35)	**<0.001**	0.29 (0.17, 0.40)	**<0.001**	0.3 (0.19, 0.42)	**<0.001**
Time x glaucoma (reference: Glaucoma)(per y.)								
Healthy	2.08 (0.09, 4.07)	**0.040**	1.61 (−0.61, 3.83)	0.155	2.99 (0.84, 5.14)	**0.006**	3.25 (1.17, 5.33)	**0.002**
Glaucoma Suspect	1.83 (0.11, 3.56)	**0.037**	1.54 (−0.58, 3.67)	0.154	3.06 (1.07, 5.05)	**0.003**	2.4 (0.44, 4.36)	**0.016**

Abbreviations: CI, confidence interval; y, years; MOPP, mean ocular perfusion pressure; SSI, signal strength index